

Angular momentum changing transitions in proton-Rydberg hydrogen atom collisions

D. Vranceanu¹, R. Onofrio^{2,3}, and H. R. Sadeghpour³

ABSTRACT

Collisions between electrically charged particles and neutral atoms are central for understanding the dynamics of neutral gases and plasmas in a variety of physical situations of terrestrial and astronomical interest. Specifically, redistribution of angular momentum states within the degenerate shell of highly excited Rydberg atoms occurs efficiently in distant collisions with ions. This process is crucial in establishing the validity of the local thermal equilibrium assumption and may also play a role in determining a precise ionization fraction in primordial recombination. We provide an accurate expression for the non-perturbative rate coefficient of collisions between protons and $H(n\ell)$ ending in a final state $H(n\ell')$, with n being the principal quantum number and ℓ, ℓ' the initial and final angular momentum quantum numbers respectively. The validity of this result is confirmed by results of classical trajectory Monte Carlo simulations. Previous results, obtained by Pengelly and Seaton only for dipole-allowed transitions $\ell \rightarrow \ell \pm 1$, overestimate the ℓ -changing collisional rate coefficients approximately by a factor of six, and the physical origin of this overestimation is discussed.

Subject headings: atomic processes — stellar astrophysics — photosphere — early universe

1. Introduction

Collisions between electrons or protons and Rydberg atoms modify the atomic level populations, enhancing or suppressing statistical equilibrium, and upsetting selection rules and

¹Department of Physics, Texas Southern University, Houston, TX 77004, USA; daniel.vranceanu@gmail.com

²Dipartimento di Fisica e Astronomia “Galileo Galilei,” Università di Padova, Via Marzolo 8, 35131 Padova, Italy, and ITAMP, Harvard-Smithsonian Center for Astrophysics, Cambridge, MA 02138, USA; onofrior@gmail.com

³ITAMP, Harvard-Smithsonian Center for Astrophysics, Cambridge, MA 02138, USA; hrsadeghpour@gmail.com

decay channels established by purely radiative transitions. Electron-H(n) collisions are more efficient in transferring energy than p-H(n) collisions, while the latter are far more effective in mixing ℓ states. Collisional capture of electrons into highly-excited states is the primary process by which atoms form in cold and ultracold plasmas, and by which anti-hydrogen atoms are created in non-neutral magnetized antiproton and positrons plasmas (Gabrielse 2005). During this stage, high- ℓ states are preferentially populated, and subsequent collisions with electrons (and ions) populate low- ℓ states that have much faster radiative de-excitation rates.

Early theoretical results for proton-hydrogen atom collisions were obtained by Demkov et al. (1974) for low quantum numbers, by Percival & Richards (1977) using a classical model, and by Abrines (1966) employing classical trajectory Monte-Carlo (CTMC) simulations. Measurements of low ℓ -mixing rates were performed for beam gas Na⁺-Na($n\ell$) collisions (Sun & MacAdams 1993) and theoretical comparison was provided via Floquet analysis (Cavagnero 1995). More recently, electron ℓ -changing collisions were shown to be responsible for transferring magneto-optically trapped rubidium Rydberg atoms into high angular momentum states (Dutta et al. 2001). In this case, electron ℓ -mixing efficiency is boosted by the presence of the trapping potential allowing for frequent collisions with the Rydberg atoms. The ℓ -changing processes are also important in Zero Electron Kinetic Energy (ZEKE) spectroscopy (Schlag & Levine 1997).

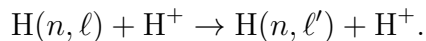
In a more strict astrophysical setting, collisional physics, both n -changing and ℓ -changing, is critical to understand the validity of the assumptions on which the determination of stellar physical parameters - such as effective temperature, density, and chemical abundances - relies (Mashonkina 1996, 2009; Bergemann 2010; Hillier 2011). The concept of thermodynamical equilibrium applicable in the stellar interior - where the mean free paths for photons, electrons, and ions is rather small with respect to their average distance - no longer holds near the surface of the star. In an intermediate regime, the photons escape with a large mean free path, while electrons and ions still maintain small mean free paths for collisions. This is the origin of a peculiar status in which, although the photon distribution departs from the equilibrium black-body distribution, the gas particles still achieve energy distribution characteristic of thermodynamic equilibrium. This allows for the evaluation of gas particle population via the knowledge of the local temperature alone, known as Local Thermodynamic Equilibrium (LTE).

However, in the upper part of the stellar atmosphere, the chromosphere, the particle densities drop so much that even collisions among the gas particles and photons are not enough for maintaining LTE. This leads to a breakdown of LTE, with the atomic populations and the ion and electron densities no longer determined by the Boltzmann and Saha

formulas, and the detailed knowledge of atomic level population for each species, including angular momentum states, is instead required (Sampson 1977). The validity and the breakdown of LTE depend upon the strength of the atomic transitions. For transitions having optical depths larger than the optical depth in the surrounding continuum, the thickness of the corresponding region is relatively small, allowing one to meaningfully use the average values for the entire region. This is not true if the line-forming region is located in the chromosphere, where the condition of LTE has to be relaxed. Collisional excitations are also important for the determination of the primordial helium abundance (Luridiana et al. 2003), the understanding of line formation for early-type stars (Przybilla & Butler 2004), and the spectroscopy of planetary nebulae (Pipher & Terzian 1969; Brocklehurst 1970; Samuelson 1970; Otsuka et al. 2011).

Moreover, the redistribution of ℓ -state populations in $H(n\ell)$ in high redshift universe can change the spectrum of the primordial recombination at low frequencies, leading to emission of successively lower-frequency photons and spectral distortion. The new surveys of the cosmic background background, such as the 7-year data integration of the WMAP satellite, and the forthcoming data from the Planck Surveyor, promise higher-precision determination of the cosmological parameters, in particular the spectral index of scalar perturbations and the baryon content of the Universe. These two parameters are directly affected by modifications to the cosmological recombination models. Mixing among high- ℓ states, for lower redshifts, leads to an increase in recombination to the ground state, while n -changing collisions suppress the emission of recombination epoch photons (Chluba et al. 2007, 2010).

In this work, we provide analytical expressions for ℓ -mixing rate coefficient in collisions between a Rydberg hydrogen atom and a proton, represented by the process:



The theoretical model can treat the more general case of collisions with an ionic projectile of mass M and charge Z . A semiclassical perturbation theory for $\ell \rightarrow \ell \pm 1$ collisions (Pengelly & Seaton 1964) is divergent for both small and large impact parameters, requiring the introduction of an *ad-hoc* radial cut-off to regularize the results. The model proposed in this paper is non-perturbative and the only assumption made is that the projectile moves on a straight line. This is well justified by the fact that collisions with large impact parameter have large probability for ℓ -changing, as first shown in Vrinceanu & Flannery (2001a). Moreover, our model predicts that the rates decrease roughly as $|\Delta\ell|^{-3}$.

2. Angular momentum changing transitions

In our model for collisions between charged particles and Rydberg atoms, we make three basic assumptions. First, we assume that collisions occur on timescales which are much longer than the orbital motion of the Rydberg electron. This implies that the Rydberg electron travels many orbitals during one collision in order to appreciably change its angular momentum. Second, we assume that the colliding particle creates a weak electric field, yet large enough with respect to the Stark electric field required to lift the hydrogenic degeneracy in each Rydberg manifold of principal quantum number n . Third, for pure angular momentum mixing without energy exchange, it is necessary that collisions occur at large impact parameters. Within the above mentioned approximation scheme, the physical picture for ℓ -changing collisions is the following. For collisions at large impact parameters, it is reasonable to assume that the charged projectile moves mostly undisturbed, along a classical straight line trajectory, creating a weak electric field (Vrinceanu & Flannery 2001a). Under the influence of this electric field, the Rydberg electron slowly precesses mixing its angular momentum state inside the degenerate shell. This collision is so weak that the angular momentum changes without any exchange of energy. Because of the long range nature of the Coulomb interaction, the cross section for this process can be very large, and indeed we will find that it is logarithmically diverging for $\Delta\ell = \pm 1$ transitions, requiring a semiclassical treatment to cure this divergence. Based on geometric arguments, it is expected that the cross section scales as $\sigma \sim \pi n^4 a_0^2$, where a_0 is the Bohr radius. The results introduced in this paper are valid for $n > 10$ (semiclassical approximation), for projectile velocities smaller than the orbital velocity of the Rydberg electron, which implies an upper bound on $n\sqrt{T} < 2.4 \times 10^4 K^{1/2}$, and for densities greater than N_{crit} as defined by Eq. (12).

2.1. Straight-line trajectory time dependent probability

Within the above mentioned approximations, the time dependent Schrödinger's equation can be analytically solved for the evolution of the states within a Rydberg shell, subject to the electric potential created by the passing charged projectile (Vrinceanu & Flannery 2001a). The key step in finding the exact solution is the observation that the angular momentum and Runge-Lenz operators generate an SO(4) symmetry group, which in turn decomposes into the direct product of two rotation groups SO(3) \otimes SO(3).

The cross section for ℓ -changing collisions within an energy shell with principal quantum number n can be written as an integral over the probability of the impact parameter as

$$\sigma_{\ell \rightarrow \ell'}^{(n)} = 2\pi \int_0^\infty P_{\ell \rightarrow \ell'}^{(n)} b db, \quad (1)$$

where the probability for making $\ell \rightarrow \ell'$ transitions has the form,

$$P_{\ell \rightarrow \ell'}^{(n)} = (2\ell' + 1) \sum_{L=|\ell' - \ell|}^{n-1} (2L + 1) \left\{ \begin{matrix} \ell' & \ell & L \\ j & j & j \end{matrix} \right\}^2 \frac{(L!)^2 (n - L - 1)!}{(n + L)!} (2 \sin \chi)^{2L} \left[C_{n-L-1}^{(L+1)}(\cos \chi) \right]^2 \quad (2)$$

where $\{\dots\}$ is a six- j symbol, L is the vector sum of ℓ and ℓ' , $C_n^{(\alpha)}$ is the ultraspherical polynomial, and $j = (n - 1)/2$. The rotation angle χ is defined as (Vrinceanu & Flannery 2001a; Flannery & Vrinceanu 2003)

$$\cos \chi = \frac{1 + \alpha^2 \cos(\Delta\Phi \sqrt{1 + \alpha^2})}{1 + \alpha^2} \quad (3)$$

where $\Delta\Phi$ is the azimuthal angle swept by the projectile, such that in a complete collision $\Delta\Phi = \pi$, and α is the scattering parameter

$$\alpha = \frac{3}{2} Z \frac{n\hbar}{m_e v b} \quad (4)$$

where m_e is the electron mass and v the initial velocity of the colliding projectile. The scattering parameter is directly related to the ratio between the maximum angular momentum allowed by the Rydberg electron and the initial angular momentum of the charged projectile. A complete derivation of the above expressions can be found in Vrinceanu & Flannery (2001a); Flannery & Vrinceanu (2003).

The probability (2) depends on the impact parameter b and the projectile velocity v through α , such that the cross section in Equation (1) can be rewritten as

$$\sigma_{\ell \rightarrow \ell'}^{(n)} = \frac{9\pi}{2} \left(\frac{Zn\hbar}{m_e v} \right)^2 I_{\ell \rightarrow \ell'}^{(n)},$$

where the velocity independent integral factor $I_{\ell \rightarrow \ell'}^{(n)}$ is determined by the initial and final states as:

$$I_{\ell \rightarrow \ell'}^{(n)} = \int_0^\infty P_{\ell \rightarrow \ell'}^{(n)}(\alpha) \frac{d\alpha}{\alpha^3} \quad (5)$$

Since the collision probability scales as $P_{\ell \rightarrow \ell'}^{(n)} \propto \alpha^{2|\ell - \ell'|}$, and the rotation angle $\chi \sim 2\alpha$ for small α , the integral factor $I_{\ell \rightarrow \ell'}^{(n)}$, and therefore the cross section, diverges for collisions in which $|\Delta\ell| = 1$, i. e. the *dipole allowed* transitions. The logarithmic singularity in the cross section for large impact parameters is well known (Pengelly & Seaton 1964) and is a reflection of the impact parameter and Born approximation. This difficulty has been addressed in Pengelly & Seaton (1964) by considering either many-body collective effects, such as the plasma screening effects or Debye shielding, or the Rydberg natural linewidth, that limits the duration of ℓ -mixing collisions.

2.2. Semiclassical probability

The non-perturbative probability $P_{\ell \rightarrow \ell'}^{(n)}$ in (2) can be computed with the desired numerical precision for a range of quantum numbers, typically $n \leq 60$, before becoming unstable due to the oscillatory behavior of the ultraspherical polynomials. In order to carry out calculations efficiently and analytically beyond intermediate Rydberg principal quantum numbers, we use the asymptotic limiting forms of the six-j coefficient and the ultraspherical polynomials, $C_n^{(\alpha)}$, and obtain analytical expressions for the rate coefficients in the limit of large quantum numbers. A derivation of these results is detailed in the Appendix. The probability for ℓ -mixing transitions in this semiclassical (SC) limit can be written as

$$P^{SC}(\ell/n, \ell'/n, \chi) = \frac{2\ell'}{\pi \hbar n^2 \sin \chi} \begin{cases} 0 & , \text{ if } |\sin \chi| < |\sin(\eta_1 - \eta_2)| \\ \frac{K(B/A)}{\sqrt{A}} & , \text{ if } |\sin \chi| > |\sin(\eta_1 + \eta_2)| \\ \frac{K(A/B)}{\sqrt{B}} & , \text{ if } |\sin \chi| < |\sin(\eta_1 + \eta_2)| \end{cases} \quad (6)$$

where K is the complete elliptic integral, $A = \sin^2 \chi - \sin^2(\eta_1 - \eta_2)$, $B = \sin^2(\eta_1 + \eta_2) - \sin^2(\eta_1 - \eta_2)$, $\cos \eta_1 = \ell/n$, and $\cos \eta_2 = \ell'/n$. The same result was obtained by Vrinceanu & Flannery (2000), based on calculating the overlap between volumes in the classical phase space.

Notice that the scattering probability is zero for $\sin \chi < |\sin(\eta_1 - \eta_2)|$, which implies a sharp cutoff for χ , and consequently for the minimum allowed value of α for which the transition is possible, α_{\min} . The integral

$$I^{SC}(\lambda, \lambda') = \int_{\alpha_{\min}}^{\infty} P^{SC}(\lambda, \lambda', \chi) \frac{d\alpha}{\alpha^3}$$

can be obtained in the semiclassical approximation and is divergence-free even for $|\Delta\ell| = 1$ transitions. Moreover, the calculation of the integral simplifies for small angular momentum transfers $\Delta\ell$. In this case, Equation (7) is obtained by writing $\cos \eta_1 = \ell/n$ and $\cos \eta_2 = (\ell + \Delta\ell)/n$ and calculating the Laurent series expansion in powers of $\Delta\ell$. In this process, we take advantage of the fact that the elliptic function at origin is $K(0) = \pi/2$ and that $\sin \chi \approx 2\alpha$ for small α . This simplified expression for transition probability can be easily integrated to obtain a non-perturbative analytical expression for the corresponding cross sections and rate coefficients, for any $\Delta\ell$.

In Figure 1, the collision probability $P_{\ell \rightarrow \ell'}^{(n)} \propto \alpha^{2|\ell - \ell'|}$ is plotted versus the impact parameter b , scaled in units of the Rydberg size $a_n = n^2 a_0$, for different approximation schemes and

a specific dipole ($\Delta\ell = 1$) transition ($n, \ell = 40, 36 \rightarrow n, \ell' = 40, 35$). We can compare the Born approximation used in Pengelly & Seaton (1964), the expression in (2), and its semiclassical approximation given by Eq. 6. The result from a direct calculation of Equation (2) contains oscillations around the base line formed by semiclassical approximation Equation (6), for most of the impact parameter range. Figure 1 shows that the probability for angular momentum mixing grows linearly with the impact parameter within the semiclassical approximation. This is a counterintuitive conclusion, since one would expect that the ability of a projectile to induce changes in a target atom would decrease as the impact parameter increases. Due to long range forces and zero energy exchange, angular momentum changing collision are most effective at large impact parameters, even for separation of several hundreds Rydberg atom radii. The semiclassical approximation falls abruptly to zero at a critical impact parameter given by the condition $|\sin \chi| < \sin(\eta_1 - \eta_2)$ in Equation (6). The quantum expression in Equation (2) has a gradual decrease to zero, eventually merging with the Born result for sufficiently large b , as b^{-2} , or α^2 . This is the source of the logarithmic singularity discussed for Equation (5).

The transition probability in Pengelly & Seaton (1964) is inversely proportional to b^2 , posing two difficulties: at small b the probability diverges and therefore it cannot be properly normalized, and at large b it leads to a divergent cross section. Therefore two cut-off parameters are required. A short cut-off R_c is introduced at the point where the transition probability is 0.5, under the assumption that for $b < R_c$ the probability has fast oscillations that average to 0.5, replacing it by a constant. The more serious divergence at large impact parameters is cured by the second cut-off, that takes into account either the finite density of the medium (plasma) where such collisions occur or the finite time of these collision due to the radiative lifetime of the Rydberg atom. Figure 1 shows that the Born cross sections overestimate the quantal and semiclassical cross sections. Our quantum calculation leads to divergent cross sections only for $\Delta\ell = \pm 1$, while the semiclassical approximation provides finite results for any transitions, without the need for a cut-off parameter.

Further simplifications, accurate for most cases of interest, occur if the scaled angular momentum ℓ/n in the semiclassical formula (6) is assumed to be a continuous parameter with values ranging between 0 and 1, and the the probability is expanded in powers of $|\Delta\ell|/n$. In this case the integral factor can be calculated term by term, starting with $1/|\Delta\ell/n|^3$, to get

$$I_{\ell \rightarrow \ell'}^{(n)} \approx \frac{1}{n} I^{\text{SC}}(\ell/n, \ell'/n) = \frac{1}{n} \frac{\ell_{<}}{\ell} \left\{ \frac{2[1 - (\ell_{<}/n)^2]/3}{|\ell'/n - \ell/n|^3} + \frac{[1 - 3(\ell_{<}/n)^2]/(3\ell_{<}/n)}{|\ell'/n - \ell/n|^2} + \mathcal{O}\left(\frac{1}{|\ell'/n - \ell/n|}\right) \right\} \quad (7)$$

where $\ell_{<} = \min(\ell, \ell')$.

In Figure 2, we compare the integral factor for transitions inside the $n = 40$ shell, starting from $\ell = 8, 20,$ and 32 and going to all possible final angular momenta. Three methods are used in this calculation: integration of the quantum formula (2), direct integration of the semiclassical result (6), and the asymptotic expansion (7), dominating small angular momentum transfers. The simple expression (7) is quite effective even for larger transfers. The next term in the expansion, proportional to $1/\Delta\ell$, is easily obtained, but it does not significantly improve the agreement with quantum calculations.

2.3. Rate Coefficients

The rate coefficient for ℓ -changing transitions in contact with ions having a Maxwell-Boltzmann distribution f_{MB} , is

$$q_{n\ell \rightarrow n\ell'} = \int v \sigma_{\ell \rightarrow \ell'}^{(n)} f_{\text{MB}}(v) dv = \left(\frac{3Zn\hbar}{m_e} \right)^2 \sqrt{\frac{\pi M}{2k_B T}} I_{\ell \rightarrow \ell'}^{(n)}$$

where M is the reduced mass of the ion-atom system, and T the temperature of the ions, hereafter assumed to be expressed in Kelvin.

By using the simplified semiclassical expression (7), the collisional rate coefficient for ion induced $\ell \rightarrow \ell'$ transitions is

$$q_{n\ell \rightarrow n\ell'}(T) = 3 \sqrt{\frac{\pi}{2}} \frac{\hbar^3}{m_e^2 e^2} \sqrt{\frac{m_e e^4}{\hbar^2 k_B T}} Z^2 \sqrt{\frac{M}{m_e}} \frac{n^2 [n^2(\ell + \ell') - \ell_{<}^2(\ell + \ell' + 2|\Delta\ell|)]}{(\ell + 1/2)|\Delta\ell|^3}. \quad (8)$$

The rate coefficient in cm^3/s is then

$$q_{n\ell \rightarrow n\ell'} = 1.294 \times 10^{-5} \sqrt{\frac{M}{m_e}} \frac{Z^2}{\sqrt{T}} \frac{n^2 [n^2(\ell + \ell') - \ell_{<}^2(\ell + \ell' + 2|\Delta\ell|)]}{(\ell + 1/2)|\Delta\ell|^3} \quad (9)$$

As expected, this rate scales as n^4 with the principal quantum number and rapidly drops with the increase in angular momentum change, as $1/|\Delta\ell|^3$, similarly to the $\Delta\ell > 1$ fitting formula in Equation (4.112) of Beigman (1995). The maximum rates are obtained for the dipole allowed transitions, $\ell \rightarrow \ell \pm 1$.

It is instructive to compare our two-body rate coefficient with the results of Pengelly & Seaton (1964), which only accounts for dipole-allowed transitions,

$$q_{n\ell}^{PS}(T) = \sqrt{\frac{\pi}{2}} \frac{\hbar^3}{m_e^2 e^2} \sqrt{\frac{m_e e^4}{\hbar^2 k_B T}} Z^2 \sqrt{\frac{M}{m_e}} D_{n\ell}^{PS} \times \ln(10) \left(\frac{1 - \gamma}{\ln(10)} + \log \frac{k_B^2 m_e}{2\pi e^2 \hbar^2} + \log \frac{T m_e}{D_{n\ell}^{PS} M} + \log \frac{T}{N_e} \right) \quad (10)$$

where $\gamma = 0.577216$ is the Euler constant, the coefficient is $D_{nl}^{PS} = 6n^2(n^2 - \ell^2 - \ell - 1)$, and N_e is the electron density expressed in cm^{-3} .

Our rate coefficient in Equation (8), summed over the two dipole transitions is

$$q_{nl}(T) = 2\sqrt{\frac{\pi}{2}} \frac{\hbar^3}{m_e^2 e^2} \sqrt{\frac{m_e e^4}{\hbar^2 k_B T}} Z^2 \sqrt{\frac{M}{m_e}} D_{nl} \quad (11)$$

where the coefficient in this case is $D_{nl} = 6n^2(n^2 - \ell^2 - 1/4\ell)$. The ratio $q_{nl}(T)/q_{nl}^{PS}(T)$ becomes a slowly varying function of n and ℓ . For example, for ($T = 3,000$ K, $N_e = 300$ cm^{-3}) this ratio is 6.98 for ($n = 50, \ell = 48$), and 6.20 for ($n = 100, \ell = 98$). The reason for which the Pengelly and Seaton formula overestimates the angular momentum changing rates lies in the Born approximation.

In order to compare the ℓ -changing collisions with radiative processes, the quantity $q_{nl}\tau_{nl}$ was introduced in Pengelly & Seaton (1964), where $q_{nl} = q_{nl \rightarrow n\ell+1} + q_{nl \rightarrow n\ell-1}$ and τ_{nl} is the radiative lifetime, which is approximately given by $\tau_{nl} \approx 10^{-10} n^3 \ell^2$ s. This quantity is the inverse of a critical density above which ℓ -changing collisions are faster than radiative decay from level $n\ell$, which in our case is expressed through the relationship (in cm^{-3})

$$N_{\text{crit}} = (q_{nl}\tau_{nl})^{-1} = 73.7 \frac{\sqrt{T/10^4 \text{K}}}{Z^2} \sqrt{\frac{m_e}{M}} \frac{(n/40)^{-9}}{(\ell^2/n^2)(1 - \ell^2/n^2)} \quad (12)$$

If scaled down by a factor of approximately six, Equation (12) agrees with previous Born results in Pengelly & Seaton (1964).

We may also compare the rates for angular momentum mixing with other processes in plasmas of astrophysical relevance, as discussed in Dalgarno (1983). Firstly, the angular momentum changing rate in collisions with electrons is smaller than the rate in collision with protons by factor of $(m_p/m_e)^{1/2} \simeq 43$. The energy changing rate due to proton collision is smaller than the angular momentum changing rate by $(\Delta n/n)^3$. This factor comes from the assumption of straight line trajectory, which implies a transition probability proportional to the square of the dipole matrix element. The matrix elements for in-shell transitions are greater than those for inter-shell transition by approximately the same factor.

The electron excitation rate coefficient depends as $\sim T^{5/6} n^{14/3}$ on the temperature T and n , while the de-excitation rate coefficient depends as $\sim T^{-1/6} n^{8/3}$ (Pohl et al. 2008). Therefore for low enough temperatures, these processes will be dominated by the proton induced ℓ -mixing. The radiative relaxation rate, represented by the inverse of the radiative life time $\tau_{nl} \approx 10^{-10} n^3 \ell^2$ s, does not depend on temperature or density. A critical electron (or proton) density can be defined such that the proton induced ℓ -mixing rate is faster than the

radiative rate (Pengelly & Seaton 1964). A near-resonant charge transfer is most efficient at projectile velocities matching the velocity of Rydberg electrons and at impact parameters in the range of $(5 - 10)n^2$ (Smith & Chupka 1995). This process is therefore unlikely for ℓ -changing collisions which occur with large probability at non-velocity matching conditions and much larger impact parameters, see Fig. 1. Our CTMC simulations confirm that, in the range of parameters considered here, the number of trajectories resulting in charge transfer are a small fraction (less than 10%) of the total number of ℓ -changing trajectories. We compare rates for these processes at different temperatures in Table 1, showing that the proton induced ℓ -changing is the fastest process over a wide range of parameters.

3. Monte Carlo Simulations

In order to confirm the range of validity of our semiclassical results in Sec. 2.3, we perform numerical simulations of proton (projectile) and $H(n\ell)$ (target) collisional ℓ -mixing and calculate the rate coefficients for these collisions with the CTMC techniques. The earliest application of CTMC technique to proton - hydrogen atom collision is reported in Abrines (1966), who calculated the classical charge transfer and ionization cross sections in p - $H(n = 1)$ collision, with the initial ground state kinetic energy sampled from a microcanonical distribution. We similarly use a microcanonical population for the Rydberg atoms with generic principal quantum number n and angular momentum quantum number ℓ . The velocities of the projectile ion and the center-of-mass of the Rydberg atoms are sampled from a Boltzmann-Maxwell distribution at temperature T . The collision is started at $t = -t_{max}$ and ends at $t = t_{max}$ where $t_{max} = \eta b/v_{12}$, where $\eta = 4$ is chosen in our simulations, and v_{12} is the relative velocity between the projectile and Rydberg atom. We perform the simulations at temperatures large enough such that the propagation time is manageable, but small enough such that energetic collisions could be neglected. All 18 conjugate degrees of freedom are propagated in time with a time-adaptive implicit Runge-Kutta integration

Table 1: Rates in s^{-1} for processes occurring in a plasma with number density 10^4 cm^{-3} and various temperatures

Process	10,000 K	1,000 K	25 K
H ⁺ angular momentum changing	6362	20119	127241
Electron de-excitation	5725	840	38.9
Electron excitation	14.7	21.6	40
Radiative relaxation	2442	2442	2442

method of forth order. The selection of trajectories for the calculation of rate coefficients is achieved by ensuring conservation of the total energy and by maintaining the on-shell energy, *i. e.* $|n' - n| < 0.5$ where n' is the effective quantum number $n' = 1/\sqrt{-2E'}$ for both the target, or the charge transferred atom, at the end of the collision. If the angular momentum of the direct or charge transferred Rydberg atom at the end of the collision is in the interval $(\ell', \ell' + 1)$, then the trajectory is counted as a collision with final angular momentum ℓ' .

Care must be exercised in the choice of impact parameter distribution, considering the large range of b values which are required for effective angular momentum mixing, as illustrated in Figure 1. According to the model, the probability for a change of $\Delta\ell$ grows linearly with b up to a maximum impact parameter $b_{max} = 3n^2\epsilon/(v|\Delta\ell|)$, and is zero for $b > b_{max}$. There are two options to address this problem; one is using the importance sampling, *i. e.* to try to get a distribution that resembles the integrand, using more points where the integrand is large, or the option of using stratified sampling, in which the integration domain is partitioned into non-equal slices, each having uniform probability distribution. For the stratified sampling at a given v_{12} , the b space is divided into intervals D_1, D_2, \dots, D_k , where each segment is defined by $3n^2\epsilon/(k + 1/2) \leq bv_{12} \leq 3n^2\epsilon/(k - 1/2)$. If our model is correct, a collision with impact parameter in a segment D_k can lead only to collisions for which $|\Delta\ell| \leq k$.

We have performed simulations for 3 cases: (a) $n = 20$, $\ell = 4$, $T = 800,000$ K, (b) $n = 20$, $\ell = 4$, $T = 400,000$ K, and (c) $n = 40$, $\ell = 8$, $T = 150,000$ K. For cases (a) and (b), we run simulations for segments D_1 to D_{10} , and D_1 to D_{19} for case (c), with 40,000 trajectories within each segment. Figure 3 shows the results of the simulations.

In order to represent the results from these cases on the same graph, we scale the rates by $6n\sqrt{\pi M/(2k_B T)}$, and the angular momenta scaled by n , $\lambda = \ell/n$, $\lambda' = \ell'/n$. By scaling with the same factor above the rate coefficient, Equation (9) can be written, in atomic units, as

$$\mathcal{R}(\lambda, \lambda') = \frac{3n}{2} I_{\ell \rightarrow \ell'}^{(n)} = \frac{\lambda_{<}}{\lambda} \left[\frac{1 - \lambda_{<}^2}{|\Delta\lambda|^3} + \frac{1 - 3\lambda_{<}^2}{2\lambda_{<}|\Delta\lambda|^2} \right] \quad (13)$$

which does not depend on temperature, and depends on n , ℓ and ℓ' only through λ and λ' .

Figure 3 shows that the ℓ -changing rate is divergent at $\ell'/n = 0.2$, because this corresponds to $|\Delta\ell| \rightarrow 0$, and decreases as $1/|\Delta\ell|^3$ for larger $\Delta\ell$. The agreement between the simulated cases and the prediction of the simple formula (9) confirms the validity of the semiclassical model. The two curves are slightly different at small $\Delta\ell$ because they actually represent the scaled rate (13) integrated over the finite bins used in the simulations. The value of the scaled bin $\delta\ell'/n$ is different for case (c). We have also verified through CTMC simulations that ℓ -changing rates for electron-Rydberg H($n\ell$) are smaller with respect to the

proton ones by a ratio $\sqrt{m_p/m_e} \simeq 40$, as expected from Equation (8).

4. Conclusions

Analytical expressions for the rate coefficient of ℓ -changing collisions between protons and $H(n\ell)$ Rydberg atoms have been derived using a non-perturbative approach free of divergences, plaguing previous results for the dipole-allowed ℓ -mixing collisions. The results have been compared to CTMC simulations over a range of temperatures of astrophysical interest. The dipole-allowed ℓ -changing collision coefficient evaluated in Pengelly & Seaton (1964) overestimates the corresponding rates by about an order of magnitude.

DV is grateful to Texas Southern University High Performance Computing Center for making the necessary computational resources available. This work was partially supported by the National Science Foundation through a grant for the Institute for Theoretical Atomic, Molecular Physics at Harvard University and the Smithsonian Astrophysical Laboratory.

Appendix: Derivation of Equation (6)

In this section, the semiclassical expression (6) is derived from Equation (2) in the limit of $n \rightarrow \infty$, and the same scaled angular momenta ℓ/n and ℓ'/n .

By using Euler-Maclaurin formula, the summation of Equation (2) is approximated by an integration such that

$$\lim_{n \rightarrow \infty} P_{\ell'\ell}^{(n)} = 2\ell'n \int_0^1 \left\{ \begin{matrix} \ell' & \ell & L \\ j & j & j \end{matrix} \right\}^2 H_{jL}^2(\chi) d\left(\frac{L^2}{n^2}\right) + \mathcal{O}\left(\frac{1}{n}\right) \quad (14)$$

where H_{jL} is the generalized character associated with the irreducible representation of the rotation group (Vranceanu & Flannery 2001b), defined by:

$$H_{jL}(\chi) = L! \sqrt{\frac{(2j+1)(2j-L)!}{(2j+L+1)!}} (2 \sin \chi)^L C_{2j-L}^{(1+L)}(\cos \chi) , \quad (15)$$

in terms of ultraspherical polynomials $C_n^{(\alpha)}$. In this section $j = (n+1)/2$.

The classical limit of the 6-j symbol was first discussed by Wigner (1959), based on the physical interpretation that the square of the 6-j symbol gives the quantum probability of

coupling 3 angular momenta j_1, j_2 and j_3 to the total angular momentum j . The corresponding classical probability is then linked to the volume of a tetrahedron that has j_1, j_2 and j_3 as edges joining at a vertex, and j, j_{12} and j_{23} as the other edges, opposing that vertex. Here j_{12} and j_{23} are the intermediate coupling angular momenta. This provides only an estimate, and the agreement is quantitative only on average over neighboring angular momenta. Heuristic arguments led Ponzano & Regge (1968) to an improved formula which takes into account the oscillations inside the classically allowed region, but which fails in the vicinity of the turning points. A rigorous derivation of these results and an uniform approximation valid over a large range of values of the angular momentum, including classically forbidden ones, is given by Schulten & Gordon (1975).

The semiclassical approximation for the square of the 6-j symbol is

$$\left\{ \begin{array}{ccc} \ell' & \ell & L \\ j & j & j \end{array} \right\}^2 \approx \left[\frac{1}{\sqrt{12\pi V}} \cos(\Theta + \pi/4) \right]^2 = \frac{1}{24\pi V} (1 + \sin 2\Theta) \quad (16)$$

and zero when $V^2 < 0$ (Ponzano & Regge 1968). The semiclassical phase Θ is defined by $\Theta = \sum_{i < k} j_{ik} \theta_{ik}$ where j_{ik} is the length of the edge opposed to edge ik and θ_{ik} is the dihedral angle between faces intersecting on the edge opposed to ik . Wigner's estimate is obtained when the oscillatory factor, from the above formula, is neglected.

Using notation $z = L/n$, $\cos \eta_1 = \ell/n$ and $\cos \eta_2 = \ell'/n$, the volume of the tetrahedron is calculated as

$$V = \frac{1}{3} j^3 \left\{ [\sin^2(\eta_1 + \eta_2) - z] [z - \sin^2(\eta_1 - \eta_2)] \right\}^{1/2} \quad (17)$$

The generalized character function H_{jL} is a solution of a differential equation,

$$\frac{d^2 H_{jL}(\omega)}{d\omega^2} + 2 \cot \omega \frac{dH_{jL}(\omega)}{d\omega} + \left[4j(4j + 1) - \frac{L(L + 1)}{\sin^2 \omega} \right] H_{jL}(\omega) = 0, \quad (18)$$

derived from the corresponding differential equation for Gegenbauer polynomials. A more convenient form for Equation (18) is obtained by setting $f = \sin \omega H_{jL}(\omega)$ and $\omega = \pi/2 + x$. The resulting equation

$$f''(x) + \left[(2j + 1)^2 - \frac{L(L + 1)}{\cos^2 x} \right] f(x) = 0 \quad (19)$$

is a one-dimensional Schrödinger equation for a particle moving between $-\pi/2 < x < \pi/2$ in a symmetric potential. A simple WKB solution for this equation can be constructed to obtain the approximation

$$H_{jL}^2(\chi) \approx \frac{1}{2 \sin \chi} \left[\sin^2 \chi - (L/n)^2 \right]^{-1/2}. \quad (20)$$

Finally, by using the approximation Equation (17) for the 6-j symbol and Equation (20) for the generalized character in summation Equation (14), a semiclassical approximation for the angular momentum changing probability is obtained as

$$P^{SC}(\ell/n, \ell'/n, \chi) = \frac{\ell'}{\pi n^2 \sin \chi} \int dz [(z - \sin^2(\eta_1 - \eta_2)) (\sin^2(\eta_1 + \eta_2) - z) (\sin^2 \chi - z)]^{-1/2}. \quad (21)$$

This is precisely the same formula obtained from purely classical phase space arguments in Vranceanu & Flannery (2001a). The integration is limited to a proper domain, where the argument of the square root function is positive, otherwise, in the classical limit, the probability for transition is zero. Moreover, the integral can be calculated in terms of the complete elliptic integral $K(m) = \int_0^{\pi/2} (1 - m \sin^2 x)^{-1/2} dx$ (formula 3.131.4 of Gradshteyn (2000)), to finally obtain the semiclassical approximation Equation (6).

REFERENCES

- Abrines, R., & Percival, I. A. 1966, Proc. Phys. Soc., 88, 861
- Beigman, I.L., & Lebedev, V.S. 1995, Phys. Rep., 250, 95
- Bergemann, M. 2010, in *Uncertainties in Atomic Data and How They Propagate in Chemical Abundances*, ed. V. Luridiana, J. Garcías Rojas, & A. Manchado (Instituto de Astrofísica de Canarias), in press (arXiv:1104.1640)
- Brocklehurst, M. 1970, MNRAS, 148, 417
- Cavagnero, M.J. 1995, Phys. Rev. A, 52, 2865
- Chluba, J., Rubiño-Martin, J.A., & Sunyaev, R.A. 2007, MNRAS, 374, 1310
- Chluba, J., Vasil, G.M., & Dursi, L.J. 2010, MNRAS, 407, 599
- Dalgarno, A, 1983, in *Rydberg States of Atoms and Molecules*, ed. R.F. Stebbings & F.B. Dunning (Cambridge University Press), 1
- Demkov, Yu.N., Ostrovskii, V.N., & Solov'ev E.A. 1974, Zh. Eksp. Teor. Fiz. 66, 125 (Sov. Phys. JETP 39, 57)
- Dutta S.K., Feldbaum, D., Walz-Flannigan, A., Guest, J.R., & Raithel G.2001, Phys. Rev. Lett., 86, 3993
- Flannery, M.R. & Vranceanu, D. 2003, Int. J. Mass Spectr., 223, 473

- Gabrielse, G. 2005, *Adv. At. Mol. Opt. Phys.*, 50, 155
- Gradshteyn, I.S., & Ryzhik, I.M. 2000, *Table of Integrals, Series and Products* (San Diego: Academic Press), 250
- Hillier, D.J. 2011, *Ap&SS*, 336, 87
- Luridiana, V., Peimbert, A., Peimbert M., & Cerviño, M. 2003, *ApJ*, 592, 846
- Mashonkina, L. 2009, *Phys. Scr.*, T 134, 014004
- Mashonkina, L.I., 1996, in *ASP Conf. Ser. 108, Model Atmospheres and Spectrum Synthesis*, ed. S.J. Adelman, F. Kupka, & W.W. Weiss (San Francisco, CA:ASP), 140
- Otsuka, M., Meixner M., Riebel D., Hyung S., Tajitsu A., & Izumiura H. 2011, *ApJ*, 729, 39
- Pengelly, R.M., & Seaton, M.J. 1964, *MNRAS*, 127, 165
- Percival, I.C., & Richards, D. 1977, *J. Phys. B* 10, 1497
- Pipher, J.L., & Terzian, Y. 1969, *ApJ*, 155, 475
- Pohl, T., Vrinceanu, D., & Sadeghpour, H.R. 2008, *Phys. Rev. Lett.*, 100, 223201
- Ponzano, G., & Regge, T. 1968, in *Semiclassical Limit of Racah Coefficients, Spectroscopic and Group Theoretical Methods in Physics* (Amsterdam, North-Holland), 100
- Przybilla, N., & Butler, K. 2004, *ApJ.*, 609, 1181
- Sampson, D.H. 1977, *J. Phys. B*, 10, 749
- Samuelson, R.E. 1970, *J. Atmos. Sci.*, 27, 711
- Schlag, E.W., & Levine, R.D. 1997, *Comments At. Mol. Phys.*, 33, 159
- Schulten, K., & Gordon, R.G. 1975, *J. Math. Phys.*, 16, 1971
- Smith, J.M., & Chupka, W.A. 1995, *J. Chem. Phys.*, 103, 3436
- Sun, X., & MacAdams, K.B. 1993, *Phys. Rev. A*, 47, 3913
- Vrinceanu, D., & Flannery, M.R. 2000, *Phys. Rev. Lett.*, 85, 4880
- Vrinceanu, D., & Flannery, M.R. 2001, *Phys. Rev. A*, 63, 032701
- Vrinceanu, D., & Flannery, M.R. 2001, *J. Phys. B*, 34, L1

Wigner, E. P., 1959, Group Theory (New York: Academic Press), 100

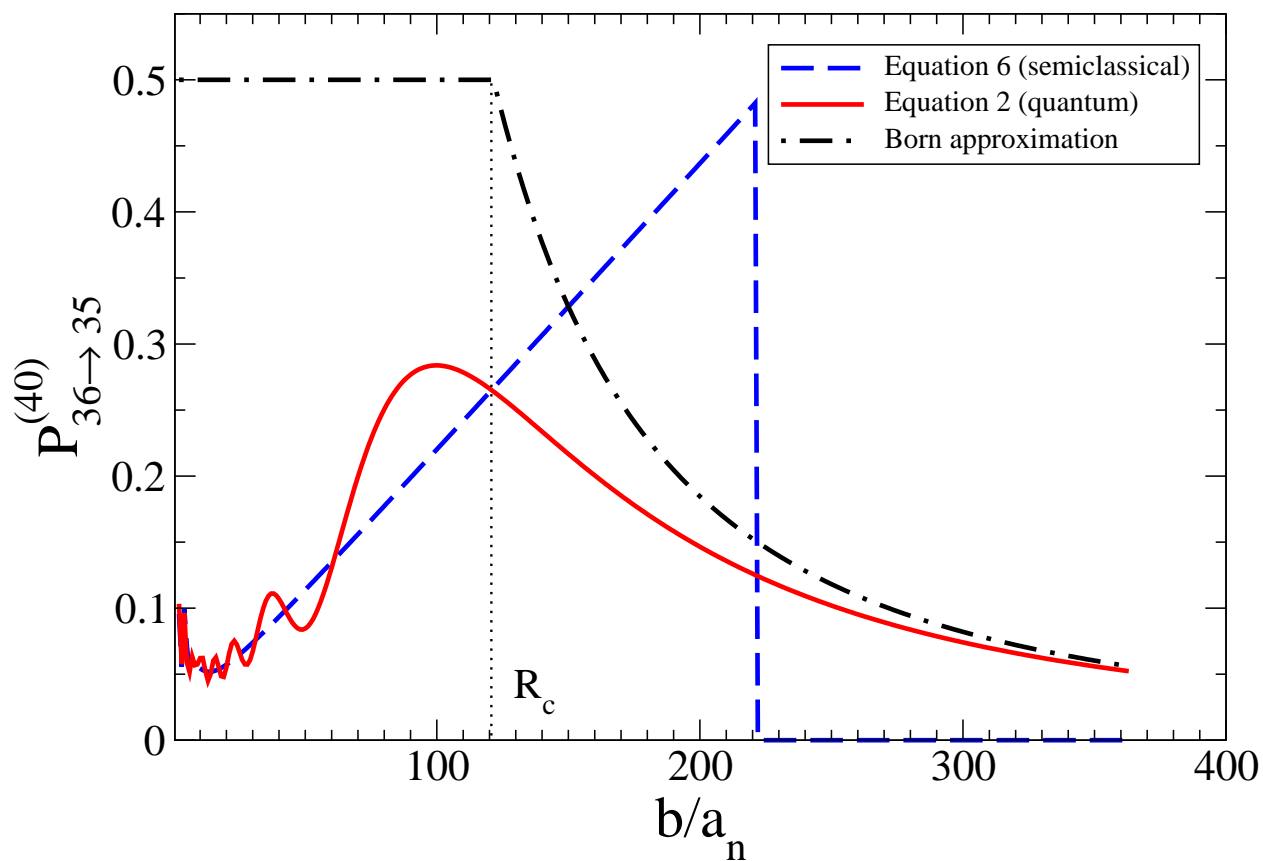


Fig. 1.— Probabilities for a dipole allowed transition in the $n = 40$ degenerate hydrogen manifold, for a $36 \rightarrow 35$ transition, as a function of the scaled impact parameter b/a_n , for a fixed projectile velocity $v = 0.1$ in atomic units, $a_n = n^2 a_0$. Exact quantum probability (red), semiclassical (blue), and Born approximations (black) are compared. The dotted line marks the position of the inner cut-off radius used in the Born approximation in Pengelly & Seaton (1964).

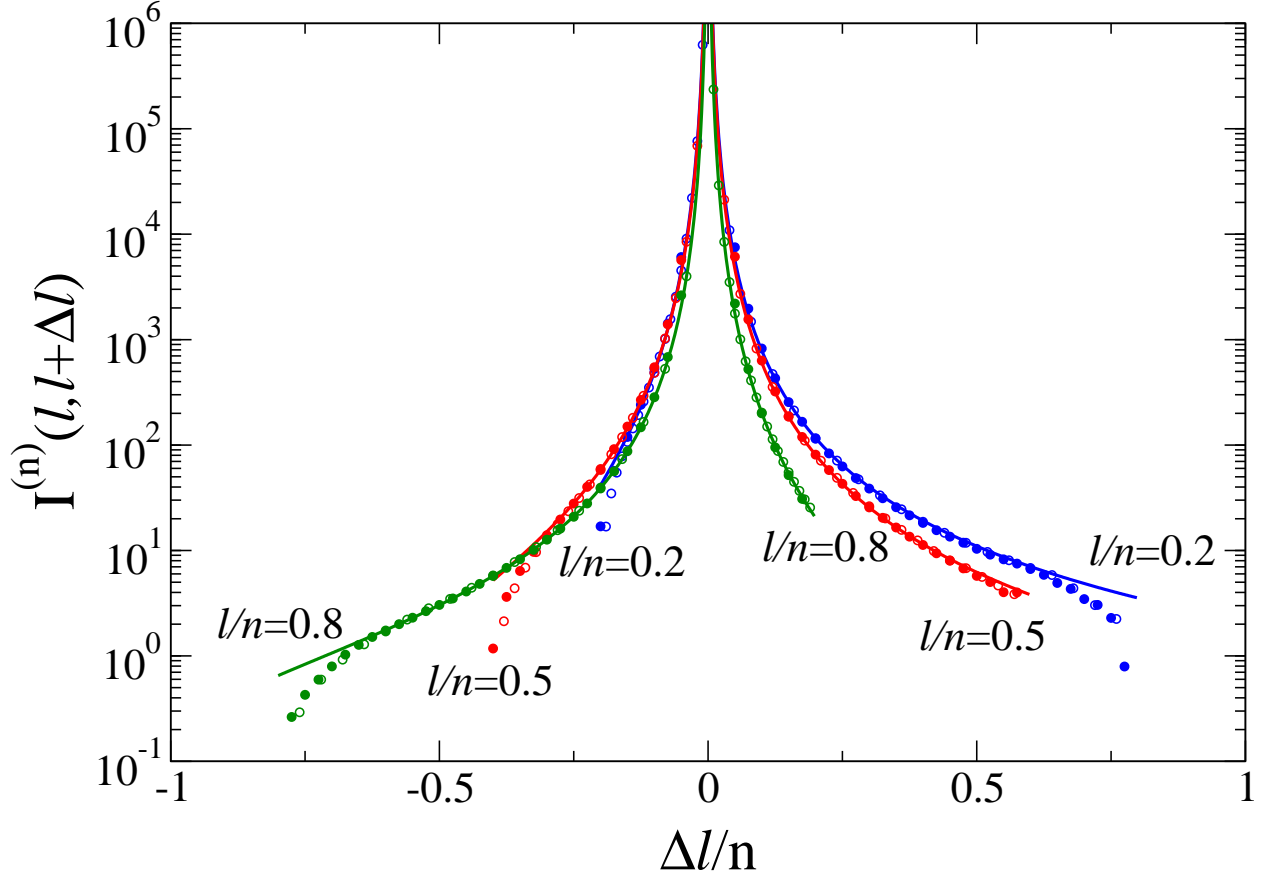


Fig. 2.— Integral factor $I_{\ell \rightarrow \ell'}^{(n)}$ in Equation (5) calculated rigorously and using a simplified semiclassical expression, as a function of the scaled angular momentum transfer. The continuous line, the empty circles, and the full circles are obtained from the expressions in Equations (7),(6), and (2), respectively.

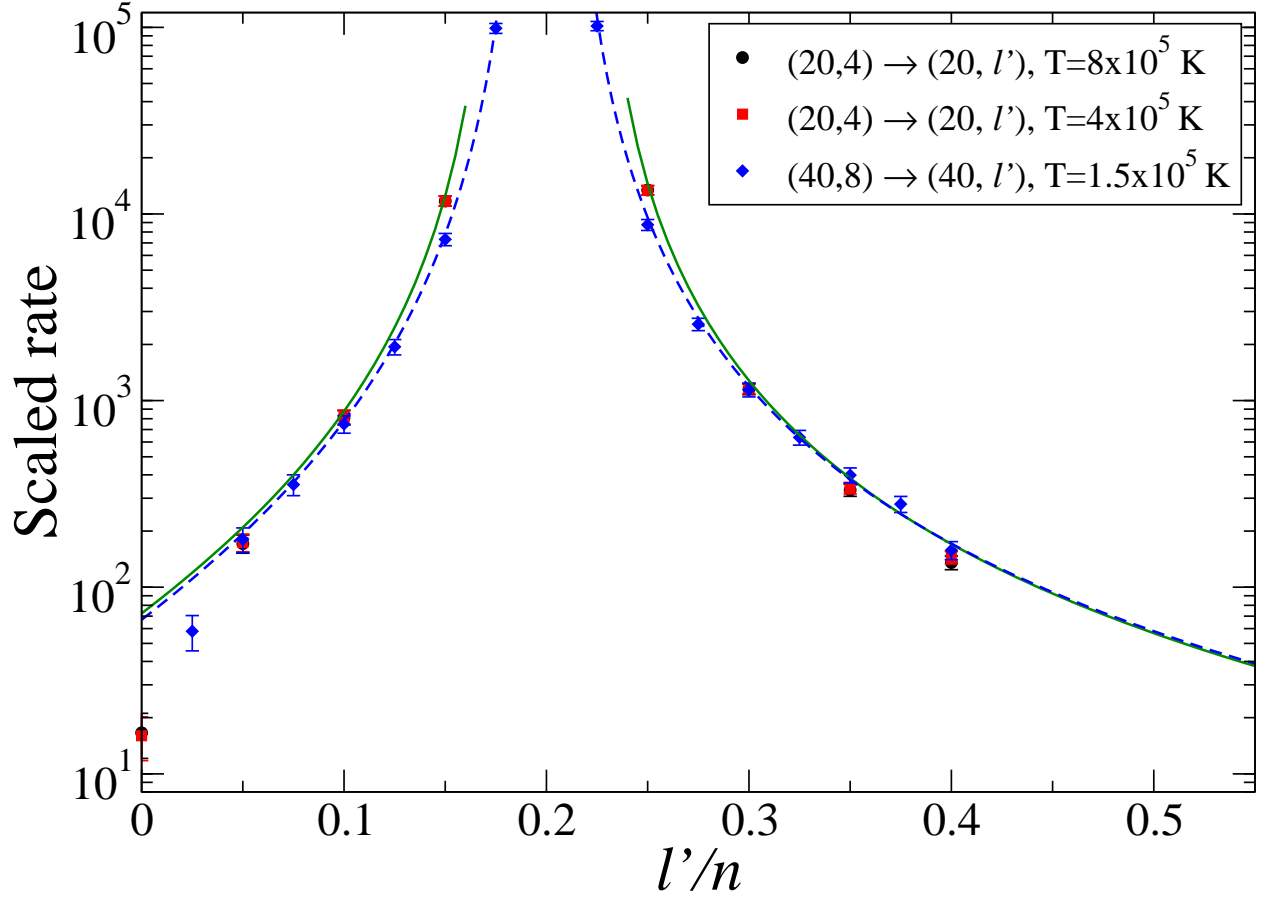


Fig. 3.— CTMC calculation of angular momentum mixing rates scaled by $6n\sqrt{\pi M/(2k_B T)}$, as a function of the scaled final angular momentum. Dots, squares, and diamonds are the results for the three cases discussed in the text, with their statistical errors. Solid lines are predictions given by Equation (13), integrated over the same final angular momentum bins used in simulations.